Creating mesopores in ZSM-5 zeolite by alkali treatment: a new way to enhance the catalytic performance of methane dehydroaromatization on Mo/HZSM-5 catalysts

Lingling Su, Lin Liu, Jianqin Zhuang, Hongxia Wang, Yonggang Li, Wenjie Shen, Yide Xu*, and Xinhe Bao**

State Key Laboratory of Catalysis, Dalian Institute of Chemical Physics, The Chinese Academy of Sciences, 457 Zhongshan Road, Dalian 116023, P.R. China

Received 2 July 2003; accepted 17 September 2003

Well-controlled treatment with alkali solution causes the etching of HZSM-5 framework, which results in the formation of the new porosity and channel structure with the coexistence of micropores and mesopores, as evidenced by nitrogen adsorption experiments. The dissolution of the zeolite framework, as revealed by the investigation of solid-state NMR, begins from the crystalline site with Si–O–Si linkages. The inertness of the alkali treatment toward Si–O–Al bond in the framework preserves the specific Brønsted acid site that is defined to be the bridging OH species over Si–O–Al units in zeolite. The Mo-modified catalysts derived from the alkali treatments showed a very high catalytic performance in the conversion of methane to aromatics (MDA) when compared with the conventional Mo/HZSM-5 catalyst. The unique selectivity to aromatics and stability of the catalysts derived from the alkali-treated ZSM-5 are attributed to the coexistence of mesopores and inherent micropores in the zeolites, which optimizes an environment for catalytic reaction and mass transfers. The channel with mainly 3–5 nm in diameters in the zeolites serves as the ''aisle'' to enhance the diffusion of molecules, especially the aromatics molecules, while the micropores have been identified to be the active cavities for the aromatics formation.

KEY WORDS: methane dehydroaromatization; Mo/HZSM-5; alkali treatment; micropore; mesopore.

1. Introduction

Great progress has been made in methane dehydroaromatization (MDA) under nonoxidative conditions during the past 10 years [1–4]. Till now, Mo/HZSM-5 is one of the best among the tested catalysts. Many features of the MDA reaction over Mo/HZSM-5 catalysts have been revealed and have become understandable. How to further facilitate the activation and conversion of methane molecules and simultaneously suppress the formation of carbonaceous deposits, so as to enhance the activity and stability of the catalyst is still a serious problem faced by catalytic chemists who are interested in the MDA reaction.

As far as a solid acid material modified with metal, such as Mo/HZSM-5, is concerned, coke formation depends mainly on the nature, distribution and number of acid sites; the distribution and state of molybdenum species; the zeolite pore structure and on the reaction temperature [5–8]. Therefore, the problem of coke formation is even much greater in the present case, since a reaction temperature as high as 973 K is necessary for the conversion of methane molecules in the MDA reaction. Nevertheless, many researchers are still trying to find an effective way through the modification of HZSM-5 zeolite and Mo/HZSM-5 catalysts to suppress coke formation during MDA reaction. The first part is the research about the effect of acidity adjustment on coke formation. Iglesia and coworkers [9] have claimed that selective silanation of external acid sites on HZSM-5 by using large organosilane molecules could decrease the content of acid sites as well as the number of MoO_x species retained at the external surface, which is regarded as a key factor for the harmful coke formation during MDA. On samples prepared with silica-modified HZSM-5, the MoO_x precursors and the active MoC_x species formed during the CH_4 reaction at 950 K were found to reside predominately within the zeolite channels, where spatial constraints could inhibit the bimolecular chain-growth pathways. Consequently, the formation rate of hydrocarbons on 4% Mo/silica-modified HZSM-5 increased by about 30% in comparison with that on 4Mo/HZSM-5 catalyst. Meanwhile, Lin and coworkers [10,11] demonstrated that significant improvements could be realized on a molybdenum catalyst supported on predealuminated HZSM-5 by steam treatment. The C_6H_6 yield increased by 32%, while the selectivity to coke dramatically dropped from 20 to 8% when compared with the unpretreated Mo/HZSM-5 catalysts. The authors suggested that the excess Brønsted acid sites in the Mo/HZSM-5 catalysts are harmful to the reaction due to the formation of coke on them. These excess

* To whom correspondence should be addressed.
E-mail: xuyd@dicp.ac.cn
** To whom correspondence should be addressed.
E-mail: xhbao@dicp.ac.cn

1011-372X/03/1200–0155/0

Brønsted acid sites can be removed via predealumination of the HZSM-5 by steam treatment. In this way, coke formation can be effectively inhibited and the benzene yield as well as the durability of the Mo/HZSM-5 catalyst increase. All these studies demonstrate that acidity adjustment of the catalysts is an effective approach for decreasing the coke deposition on the catalysts during the reaction and thus for prolonging the catalyst life.

Secondly, adjusting the distribution of molybdenum species (on the external surface or in the channel of the catalyst) and the type of the active center of Mo_2C (α-MoC_{1-x} or β-Mo_2C) is also very effective for prolonging the catalytic life. Iglesia reported that molybdenum species would migrate into the channel during calcination between 773 and 973 K, and they got a better reaction result on Mo/HZSM-5 catalyst after the special calcination process (about 8% methane conversion after 10 h) [12]. Bouchy *et al*. have reported that the activation of the Mo-oxide/H-MFI precursor with an *n*-butane/hydrogen mixture resulted in higher catalyst stability and benzene selectivity. And they suggested that the active center of the classical catalyst described in previous research was β-Mo_2C, while by activating the Mo-oxide/H-MFI precursor with an *n*-butane/hydrogen mixture α-MoC_{1-x} with fcc structure was formed. α-MoC_{1-x} showed superior performance: higher activity, higher selectivity to benzene and higher stability compared with β-Mo_2C [13,14].

Owing to the obvious difference in the molecule size of the reactant (methane) and the products (mainly benzene and naphthalene) in MDA, pore-size distribution and channel structure of the zeolites may also play an important role from the point of view of shape selectivity and mass transport in the zeolite channels [15]. But until now, the research about the effect of pore structure of the catalyst on reaction performance and coke formation has not been reported. It has been reported recently that proper alkali modification to the MFI zeolite is an effective method to change its pore-size distribution and to create a kind of secondary mesopores [16–19]. By using this alkali-treated MFI zeolite, the activity and selectivity of the cumene cracking has been enhanced a lot, in spite of the fact that the acidity of the alkali-treated zeolite has only changed very little quantitatively or qualitatively. Alkali treatment removes mainly the silicon from the zeolite, thus creating extraporosity, which is favorable for overcoming the diffusion limitation to some extent. In the present work, the NH_4ZSM-5 zeolite was first treated with a NaOH solution of desirable concentration for appropriate time, followed by ion exchange with an NH_4OH solution. The sample was then used to prepare a 6 wt% Mo/HZSM-5 catalyst. In this way, a remarkable improvement in the catalytic performance for MDA over the alkali-treated 6Mo/HZSM-5 catalyst was obtained. The selectivity to coke decreased from 33 to 13% and the aromatics yield increased from 1.7 to 9.3% after running the reaction for 720 min, as compared with the conventional 6Mo/HZSM-5 catalysts under a reaction temperature of 1003 K. The results demonstrate that alkali treatment is also an effective way for enhancing the activity and stability of Mo/HZSM-5 catalysts in MDA process.

2. Experimental

2.1. Catalyst preparation

NH_4ZSM-5 with a Si/Al ratio of 25, supplied by Nankai University, was used as the parent zeolite denoted as HZSM-5(P). NH_4ZSM-5 was added to an aqueous NaOH solution and stirred for appropriate time under a given temperature. The conditions of alkali treatment of HZSM-5(P), i.e., the concentration of sodium hydroxide solution(M), temperature(K), time(h) were set at 0.05, 323, 1 denoted as AT1 and 0.2, 353, 5 denoted as AT2, respectively. After filtering and drying, the zeolite was ion exchanged with NH_4OH solution to obtain the NH_4^+ form zeolite. The NH_4^+ form zeolite was calcined at 773 K to form HZSM-5 zeolite. Mo-containing catalysts (Mo wt% = 6%, hereafter 6 wt% Mo/HZSM-5 was simplified as 6Mo/HZSM-5) were prepared by incipient wetness impregnation of the HZSM-5(P, AT1 and AT2) with an aqueous solution of ammonium heptamolybdate. After impregnation, the catalysts were dried at 383 K for 4 h and then calcined in air at 773 K for 4 h. The catalysts were crushed and sieved to 40–60 mesh granules for further use.

2.2. Catalytic evaluation

The reaction was carried out in a quartz tubular fixed-bed reactor at atmospheric pressure and 1003 K, a space velocity of 1500 $mL/g_{cat}/h$, as described in previous works [20]. The products were analyzed by an on-line gas chromatograph (Shimadzu GC-9A) equipped with a flame ionization detector (FID) for the analysis of CH_4, C_6H_6, C_7H_8 and $C_{10}H_{12}$ and a thermal conductivity detector (TCD) for the analysis of H_2, N_2, CH_4, CO, C_2H_4 and C_2H_6. A feed with 11.45% N_2 was used as an internal standard for analyzing all products, including carbonaceous deposition on the basis of converted methane molecules.

2.3. Catalyst characterizations

XRD patterns were obtained with a Rigaku D/MAX-RB X-ray diffractometer, using Cu Kα radiation at room temperature and instrumental settings of 40 kV and 100 mA. The powder diffractograms of the samples were recorded over a range of 2θ values from 5° to 50°. The scanning rate was set at 5°/min.

XRF experiments were performed on a Philips MagiX X-ray fluorescence spectrometer and an IQ+ standardless quantitative software was applied for analysis.

The morphology of the samples was observed by HITACHI H-6010 scanning electron microscopy (SEM). The zeolite samples were coated with gold prior to the SEM observation to avoid charge effect of the samples.

N_2 adsorption and desorption experiments were carried out at liquid nitrogen temperature using an AUTOSPRB-1 Micromeritics equipment. A value of 0.162 nm^2 for the cross-sectional area of N_2 was used. Micropore distributions were derived from the H-K method, while mesopore distributions were derived from the BJH method.

Multinuclear MAS NMR experiments were carried out at 9.4 T on a Bruker DRX-400 spectrometer using 4-mm ZrO_2 rotors. ^{29}Si MAS NMR spectra were recorded at 79.5 MHz. The magic angle-spinning rate for all ^{29}Si spectra was 4 kHz, and the chemical shifts were referenced to 4,4-dimethyl-4-silapentane sulfonate sodium (DSS). ^{27}Al MAS NMR spectra were recorded at 104.3 MHz and the samples was spun at 4 kHz. 1% $Al(H_2O)_6^{3+}$ was used as reference of chemical shifts. ^1H MAS NMR spectra were collected at 400.1 MHz. The sample was spun at 8 kHz and 200 scans were accumulated for each spectrum. The chemical shifts were referenced to a saturated aqueous solution of DSS. ^1H and ^{29}Si MAS NMR spectra were deconvoluted by a software offered by the Bruker Co. Prior to the ^1H MAS NMR experiment, the samples were first dehydrated at 673 K for 24 h in a homemade apparatus for removing the water adsorbed on the samples, then the treated samples were put into the NMR rotors for measurement, without exposing to air.

NH_3-TPD experiments were carried out as follows. The sample (0.14 g) was dried in flowing helium (99.99%, 30 mL/min) at 873 K for 0.5 h prior to NH_3 adsorption. NH_3 adsorption took place at 323 K until saturation, and then, the catalyst sample was flushed with helium at the same temperature for 1 h. TPD measurements were conducted from 323 K to 900 K, with a heating rate of 15 K/min. A thermal conductive detector (TCD) was used to monitor the desorbed NH_3 during the TPD course.

XPS experiments were recorded from a modified Leybold LHS 12 MCD system equipped with UPS, XPS and ISS, using Al Kα radiation. A software was used for data acquisition and analysis. All the binding energies were referenced to the Si(2p) peak at 103 eV. And the near-surface compositions of the sample were calculated from the peak areas using appropriate sensitivity factors, respectively.

TPO experiments were performed in a quartz tubular fixed-bed reactor equipped with an on-line quadruple-mass spectrometer (Balzers, QMS 200). The catalyst charge was 0.15 g. It was first reacted with CH_4 at 1003 K for 6 h, then cooled to room temperature and flushed with a 10% O_2/He mixture (20 mL/min) for 1 h. The temperature was raised from 303 to 1023 K at a heating rate of 8 K/min during which the m/e intensities for 44 (CO_2), 28 (CO) and 18 (H_2O) were recorded.

3. Results and discussion

3.1. Comparative study of the HZSM-5 zeolites before and after alkali treatment

3.1.1. Morphological differences

Figure 1 shows the XRD patterns of the HZSM-5 samples before and after alkali treatment. It seemed that

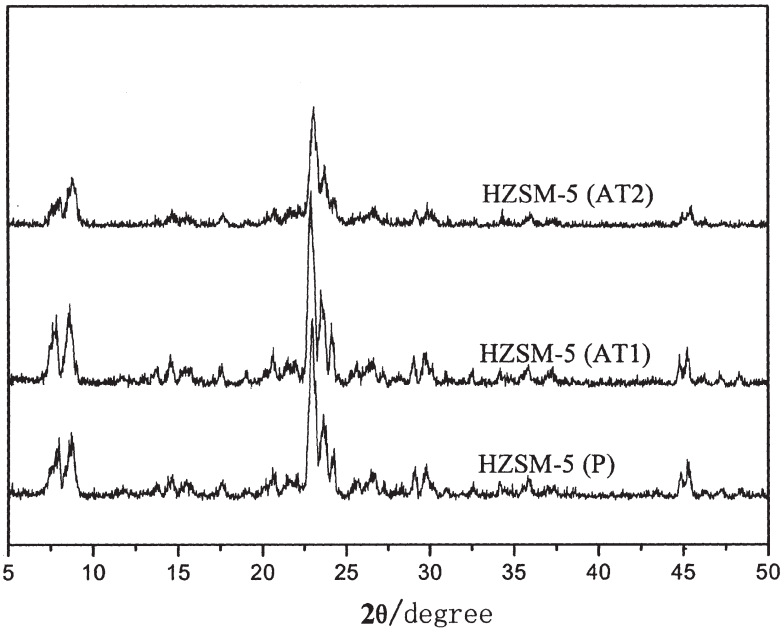

Figure 1. XRD patterns of the HZSM-5 samples before and after alkali treatments.

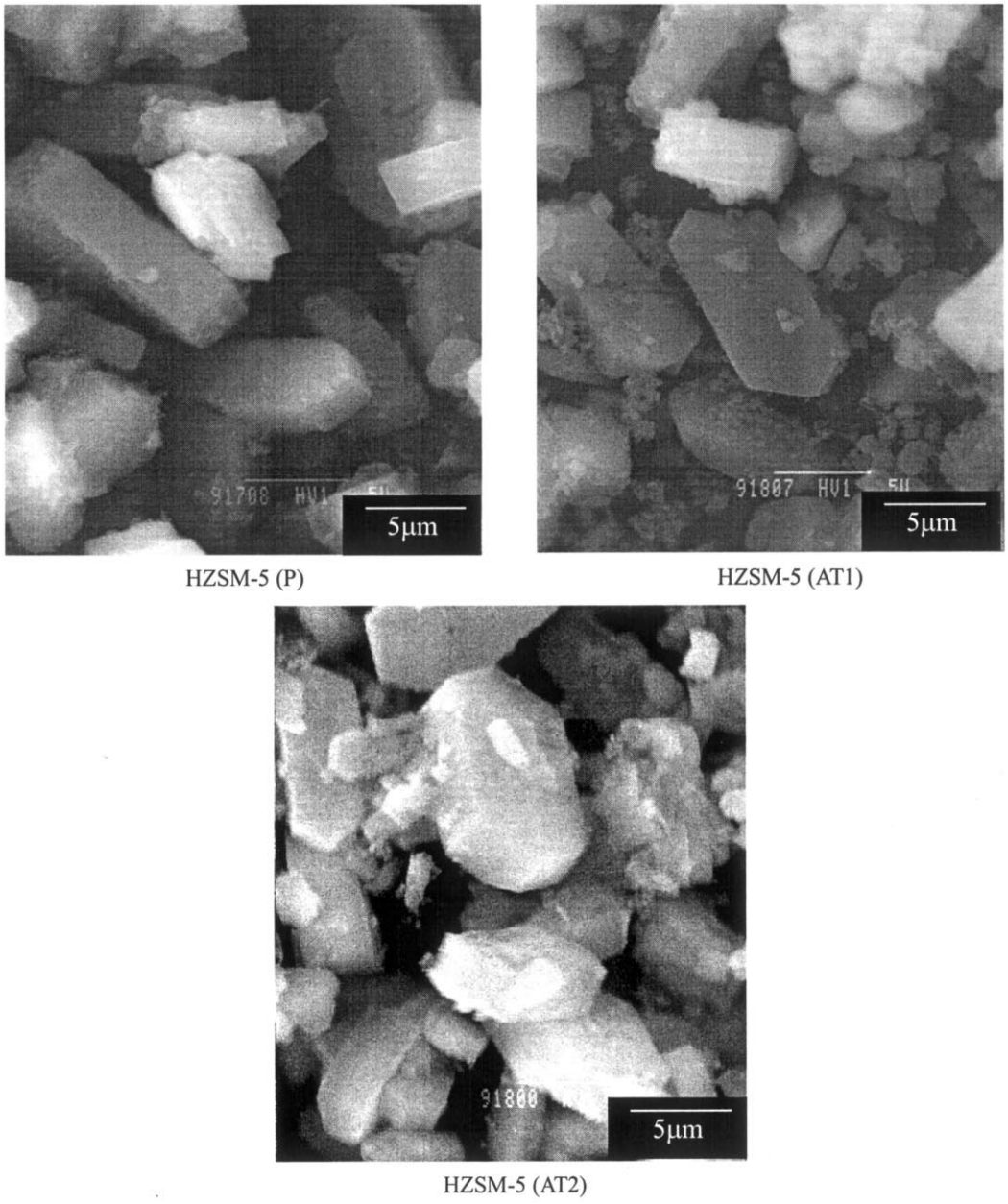

Figure 2. SEM images of the HZSM-5 samples before and after alkali treatments.

the alkali treatment did not lead to an obvious change of the crystalline phases. After the alkali treatment, the samples basically preserved the lattice structure of the HZSM-5 zeolite, except that the crystallization of the HZSM-5(AT2) sample decreased noticeably. The SEM images obtained from the alkali-treated and untreated ZSM-5 are shown in figure 2. Some crucial changes on the HZSM-5 samples occurred after the alkali treatment. Many small crystallites could be observed on the surface of the ZSM-5 particles after a moderate alkali treatment (HZSM-5(AT1)), and large HZSM-5 crystallites seemed to be dissolved and cracked by the alkaline solution into small particles. The more harsh the condition applied, the more evident change was observed.

3.1.2. Changes in the framework structure of the zeolite studied by ^{29}Si and ^{27}Al MAS NMR

Figure 3 illustrates the ^{29}Si MAS NMR spectra of the HZSM-5 samples before and after the alkali treatment. There are four peaks in the spectra recorded from the zeolite after deconvoluting the spectra by the software of Bruker WIN NMR. The peaks at $\delta = -114$ and -108 ppm can be attributed to Si(0Al) and Si(1Al) species respectively. And the signal at $\delta = -117$ ppm is related to the crystallographically inequivalent Si(0Al) sites, while the signal at $\delta = -103$ ppm is normally associated with silanol group ($(OSi)_3SiOH$) [21]. The ^{29}Si MAS NMR spectra recorded from the alkali-treated HZSM-5, i.e., HZSM-5(AT1) and HZSM-5(AT2) samples showed great changes. In the ^{29}Si

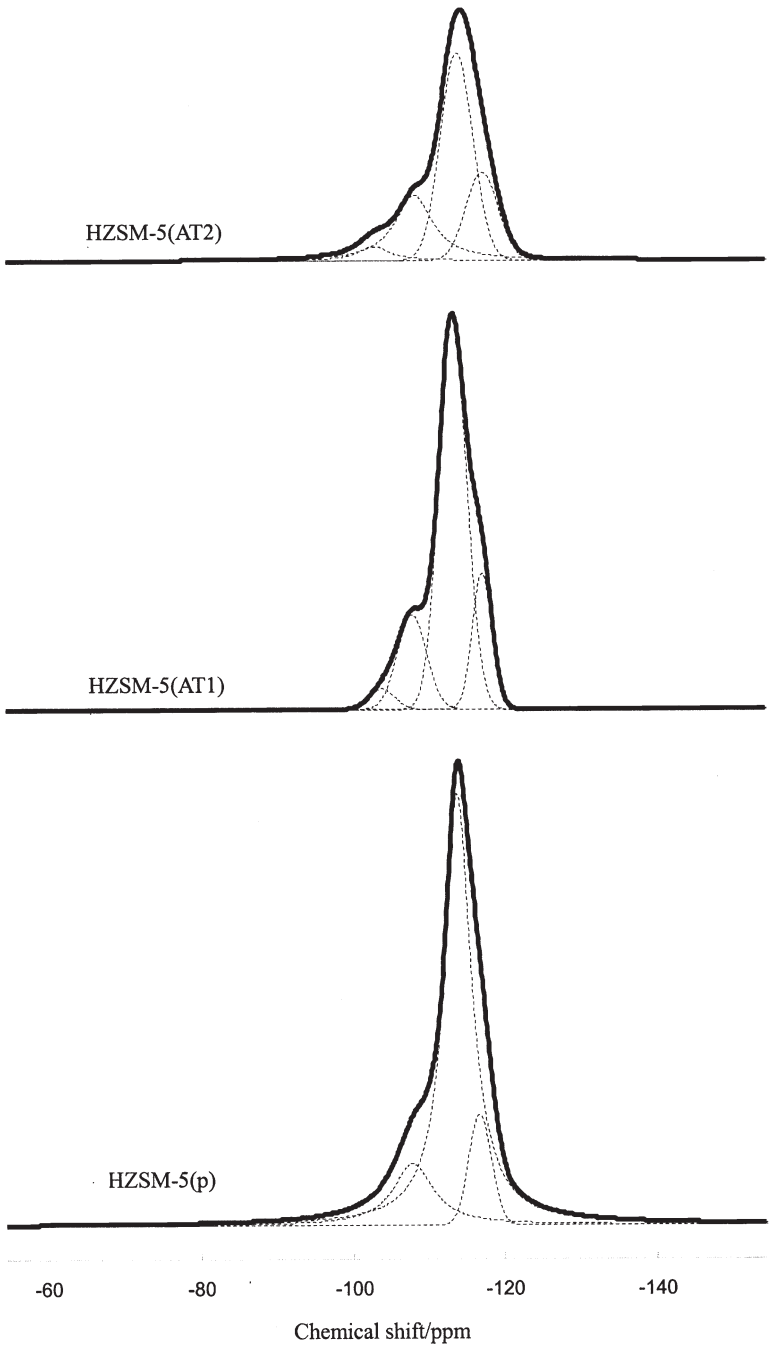

Figure 3. ^{29}Si MAS NMR spectra of the HZSM-5 samples before and after alkali treatments.

MAS NMR spectra of alkali-treated HZSM-5, the intensity of the peak at about $\delta = -114$ ppm presenting the Si(0Al) species decreased, indicating that part of the siliceous species was removed from the zeolite framework after alkali treatment, which had been pointed out by other researchers [16–19]. On the basis of the result of the ^{29}Si MAS NMR spectra, the framework Si/Al of the HZSM-5 samples before and after alkali treatment was calculated and the results are listed in table 1. The Si/Al ratio of HZSM-5(P) zeolite was 25.9 (the nominal Si/Al ratio is 25), which decreased to 24.3 after a moderate alkali treatment (HZSM-5(AT1)), and further decreased to 15.4 after a severe alkali treatment (HZSM-5(AT2)). From the above results, we can conclude that the process of alkali treatment does affect the environment of the framework silicon and leads to the dissolution of the siliceous species.

^{27}Al MAS NMR spectra of the HZSM-5 before and after alkali treatment are shown in figure 4. For the HZSM-5(P) zeolite sample, there are two bands: one is centered at ca. $\delta = 55$ ppm and the other is at ca. $\delta = 0$ ppm. The former is attributed to the framework aluminum and the latter is associated with the nonframework aluminum. For the alkali-treated

Table 1
The deconvolution results of ^{29}Si MAS NMR spectra obtained on the HZSM-5 samples before and after alkali treatments

	−103 silanol (area %)	−108 Si(1Al) (area %)	−114 Si(0Al) (area %)	−117 Si(0Al) (area %)	Si/Al
HZSM-5(P)		15	74	11	25.9
HZSM-5(AT1)	3	16	65	16	24.3
HZSM-5(AT2)	5	26	49	20	15.4

HZSM-5(AT2), the intensity of the main band at ca. $\delta = 55$ ppm decreased a little, while the intensity of the band corresponding to the nonframework aluminum increased slightly. It seemed that a slight dealumination of the zeolite framework aluminum occurred after the severe alkali treatment. While for the moderate alkali treatment, i.e., HZSM-5(AT1), the framework aluminum was not affected. All these results demonstrate that the alkali solution attacks preferentially the siliceous species of the zeolite framework and leads to its

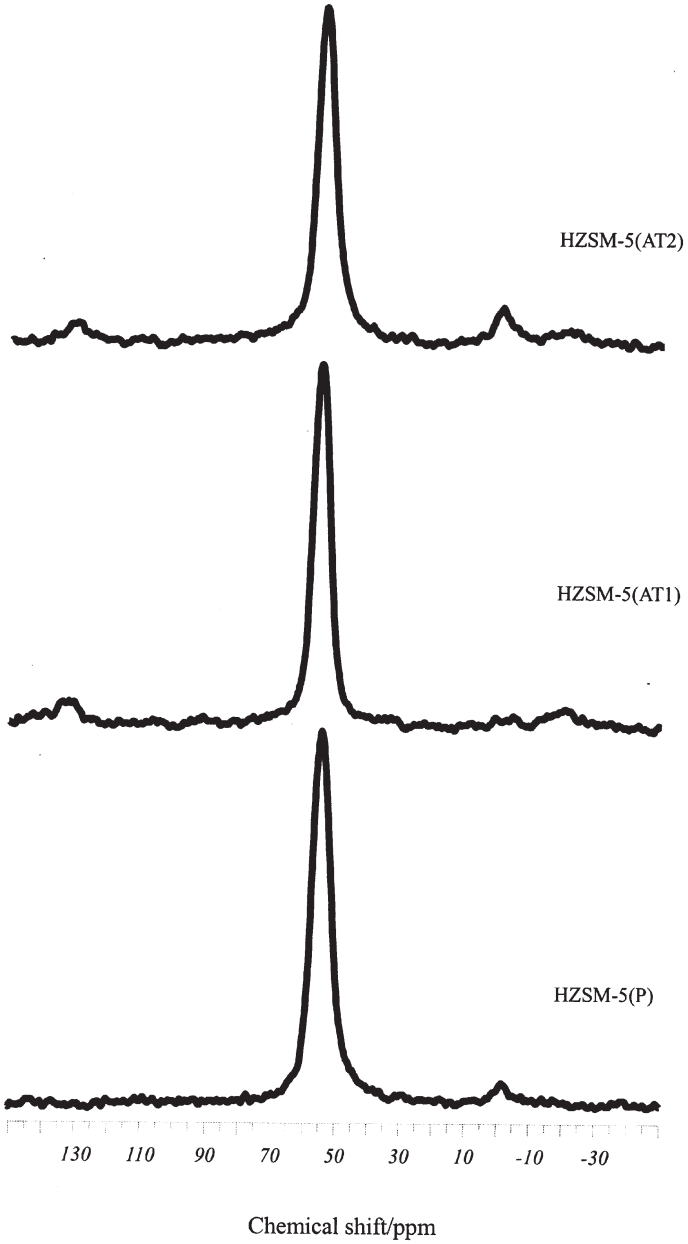

Figure 4. ^{27}Al MAS NMR spectra of the HZSM-5 samples before and after alkali treatments.

dissolution, while for aluminum species on the zeolite the alkali solution is relatively inert under the present conditions.

3.1.3. Effect of the alkali treatment on the acidity of the HZSM-5 zeolites

^{1}H MAS NMR spectra of HZSM-5(P), HZSM-5(AT1) and HZSM-5(AT2) are shown in figure 5 and the corresponding deconvolution result are listed in table 2. Five peaks at about $\delta = 1.7$, 2.2, 3.7, 4.6 and 5.8 ppm, respectively, can be clearly resolved, which are almost the same as in our previous report [22]. Accordingly, the bands at ca. $\delta = 1.7$ and 2.2 ppm are attributed to silanol group and Al–OH species respectively. The band at about $\delta = 3.7$ ppm is associated with free-bridging OH groups (Brønsted acid sites), which are perhaps in the intersection position of the channels. The resonance at ca. $\delta = 5.8$ ppm is commonly assigned to another kind of Brønsted acid sites, which is influenced by additional electrostatic interaction of the zeolite framework, i.e., the restricted Brønsted acid sites. There were no obvious changes on the HZSM-5(AT1) sample when compared with the HZSM-5(P) sample (see table 2). For the alkali-treated HZSM-5(AT2), because of the collapse of part of the zeolite framework, the number of silanol group and Al–OH species increased obviously. However, there was only a little increase in the number of free-bridging OH groups (Brønsted acid sites), accompanied by a decrease in the number of the restricted Brønsted acid sites. In other words, the results demonstrated that with the collapse of part of the zeolite framework, most of the silicon species and a small part of framework aluminum, which were originally related to the restricted Brønsted acid sites, changed into silanol group and Al–OH species that were exposed to external surface. And, at the same time, the number of free Brønsted acid sites increased slightly. In conclusion, the results of ^{1}H MAS NMR spectra of the HZSM-5 samples before and after the alkali treatment demonstrated that alkali treatment did not affect the acidity of the zeolite in terms of the amount of free Brønsted acid sites and the strength of the Brønsted acid sites.

3.1.4. A further study on the change of pore structures of HZSM-5 samples caused by the alkali treatment

BET surface area, microareas and micropore volumes of the HZSM-5 samples before and after the alkali treatment are listed in table 3. For the alkali-treated HZSM-5(AT2), the total pore volume increased from 0.2 to 0.51 cm^3/g, while the micropore volume decreased from 0.11 to 0.08 cm^3/g when compared with the HZSM-5(P) sample. On combining the changes in both total and micropore volumes with the change in the SEM images caused by the alkali treatment, it is clear that after the alkali treatment, the mesopore system has been created, while the micropore system of the zeolite has not been affected too much. The N_2-adsorption isotherm of HZSM-5(P), HZSM-5(AT1) and HZSM-5(AT2) are shown in figure 6. There was a progressive increase in the uptake for the other two samples when HZSM-5(P) was taken as basis. It is interesting to note that there was a dramatic increase in the amount of N_2 adsorption on the HZSM-5(AT2) sample. In addition, there was also a very distinct hysteresis loop on its desorption isotherm, which is characteristic of the existence of mesopores. As a consequence, the total pore volume of HZSM-5(AT2) had about twofold increase in comparison with that of HZSM-5(P).

The mesopore distribution results of HZSM-5 samples before and after alkali treatments are also illustrated in figure 6. The volume of mesopores of the alkali-treated HZSM-5 samples increased obviously. In addition, the stronger the alkali treatment condition of the HZSM-5 zeolite, the larger the volume of mesopores was. This again leads to the conclusion that after alkali treatment a kind of new mesopores is created on the zeolite. When the condition was mild (i.e. AT1), the micropore of the zeolite was not affected obviously and the mesopores formation was small. But when the alkali condition was too severe (i.e. AT2), the micropore part had been reduced and there were more mesopores formed. Thus with the alkali treatment condition becoming more and more severe, the mesopores part possessed more proportion on the all zeolite.

This change in the pore structure of the zeolite after the alkali treatment is due to the fact that the siliceous species residing along the boundaries of the MFI crystallite or in the framework will be dissolved during the alkali treatment, thus leading to the formation of secondary mesopores. The dissolution of siliceous species, caused by the alkali treatments, probably starts preferentially in positions where the crystallization is poor, such as at the boundaries or defects of the HZSM-5 zeolite crystallite.

3.2. Catalytic evaluation of 6Mo/HZSM-5(P), 6Mo/HZSM-5(AT1) and 6Mo/HZSM-5(AT2) catalysts

The catalytic behaviors for MDA on 6Mo/HZSM-5 (P, AT1 and AT2) catalysts after running the reaction for 60 and 720 min at 1003 K are listed in table 4. The change of methane conversion and aromatics yield on 6Mo/HZSM-5(P) and 6Mo/HZSM-5(AT1) catalysts with the time onstream are shown in figure 7. In the early stage of the reaction (after running the reaction for 60 min), the activities and product distributions on these three catalysts were similar. However, the 6Mo/HZSM-5(AT1) catalyst, which was prepared with HZSM-5 zeolite subjected to a moderate alkali treatment, was the most active one. Meanwhile, the 6Mo/HZSM-5(AT2) catalyst, which was prepared with the HZSM-5 zeolite that experienced a strong alkali treatment, was the least active one among the tested catalysts. Moreover, the

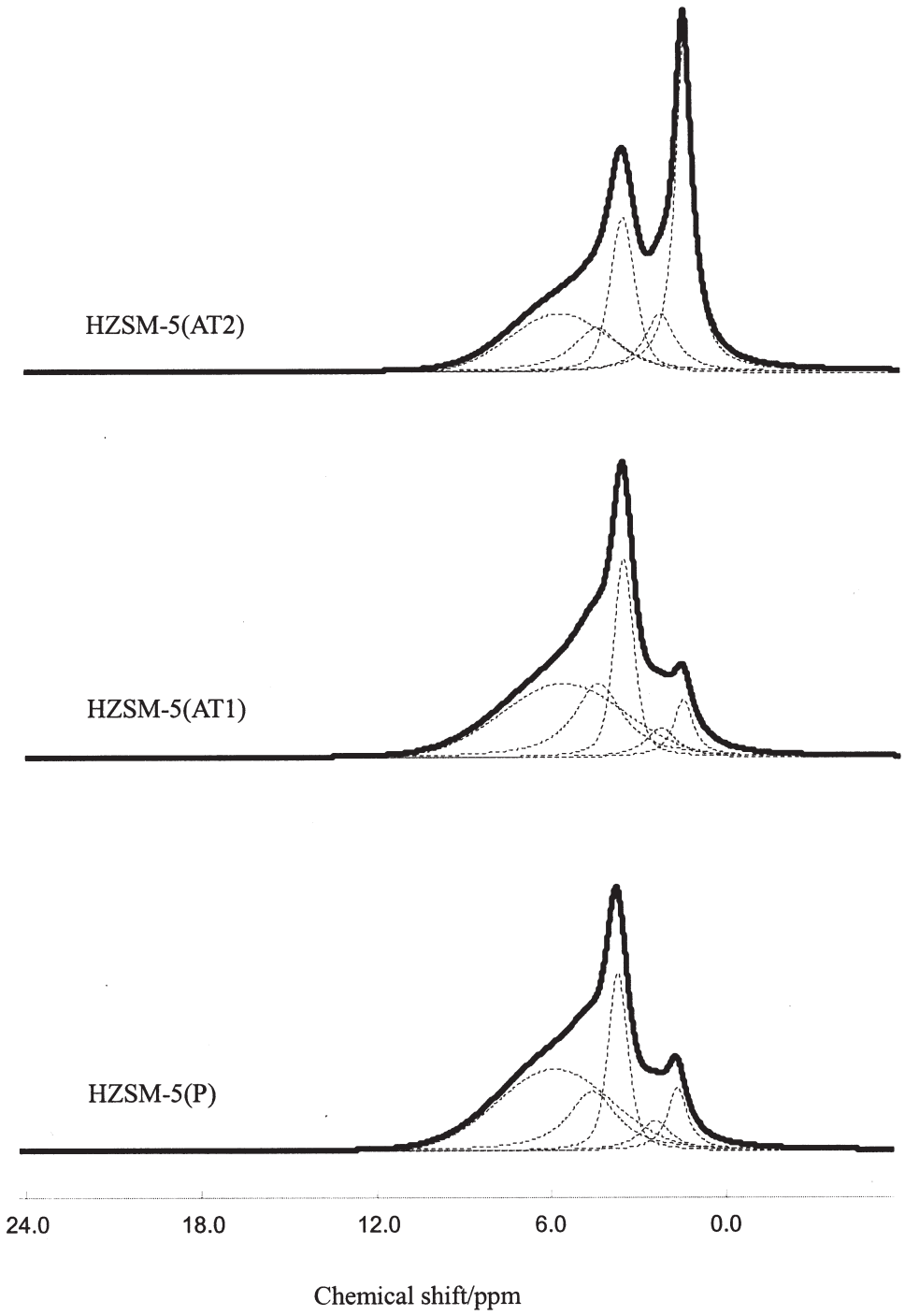

Figure 5. ^{1}H MAS NMR spectra of the HZSM-5 samples before and after alkali treatments.

Table 2
The number of different hydroxyls per unit cell estimated from ^{1}H MAS NMR spectra of HZSM-5 before and after alkali treatment

	Number of hydroxyls per unit cell				
	Si–OH $\delta = 1.7$	Al–OH $\delta = 2.4$	Al–OH–Si $\delta = 3.8$	Water $\delta = 4.6$	Second Brønsted acid $\delta = 5.8$
HZSM-5(P)	0.47	0.35	1.13	1.08	2.44
HZSM-5(AT1)	0.46	0.35	1.27	1.35	2.41
HZSM-5(AT2)	2.19	0.70	1.23	0.81	1.54

Table 3
BET surface areas and pore volumes of the HZSM-5 samples before and after alkali treatments

	S_{BET} (m^2/g)	S_{micro} (m^2/g)	V_{total} (cm^3/g)	V_{micro} (cm^3/g)
HZSM-5(P)	282	–	0.20	0.11
HZSM-5(AT1)	328	265	0.26	0.12
HZSM-5(AT2)	377	173	0.51	0.08

changes of the catalytic performances of these three catalysts with the time onstream were noticeably different. For the 6Mo/HZSM-5(P) catalyst, deactivation was very serious, and the CH_4 conversion decreased from 16.7 to 3.9% after 720 min. However, for the 6Mo/HZSM-5(AT1) catalyst, the CH_4 conversion was still as high as 11.6% after 720 min onstream. The product distributions for MDA on these two catalysts were also quite different after running the reaction for 720 min. The selectivity of C_6H_6 was ca. 68% on the 6Mo/HZSM-5(AT1), as compared with that of ca. 37% on the 6Mo/HZSM-5(P). At the same time, the formation of coke and the C_2 hydrocarbons were effectively suppressed. The selectivity to coke was ca. 33% for the 6Mo/HZSM-5(P), and was only 13% for the 6Mo/HZSM-5(AT1). It was this obvious suppression of coke formation that led to a remarkable increase in the aromatics yield from ca. 1.7% for 6Mo/HZSM-5(P) to ca. 9.3% for 6Mo/HZSM-5(AT1) after 720 min onstream. These results demonstrate that if Mo/HZSM-5 catalysts are prepared with a proper alkali-treated HZSM-5 zeolite, the catalytic activity and stability will be enhanced greatly. But if the alkali treatment condition is too severe, the reaction activity not only cannot be enhanced but is also decreased, for example, 6Mo/HZSM-5(AT2) catalyst.

3.3. *The effect of the coexistence of mesopores and micropores on the catalytic performances of MDA on alkali-treated 6Mo/HZSM-5 catalysts*

What is the reason that leads to the difference of reaction performance on the catalysts before and after alkali treatment? As is well known, the channel structure, acidity of the catalyst and the valence and location of the molybdenum species on/in the zeolite are crucial factors for its good catalytic performance of MDA on Mo/HZSM-5 [2–4].

Figure 8 shows the chemical state of molybdenum species on the surface of the catalyst by XPS technique, and table 5 presents the total chemical composition and surface chemical composition of the catalyst by XRF and XPS respectively. XRF results demonstrated that the total molybdenum content on the catalyst was not affected by the process of alkali treatment, and on these three catalysts the total molybdenum content was all equal to about 6 wt%, which was the nominal value. The valence state of molybdenum species and the near-surface chemical composition on both 6Mo/HZSM-5 and alkali-treated 6Mo/HZSM-5 samples were studied by the XPS technique. As shown in figure 8, the binding energies of Mo(3d) for the fresh alkali-treated 6Mo/HZSM-5 sample were in doublet centering at 232.9 and

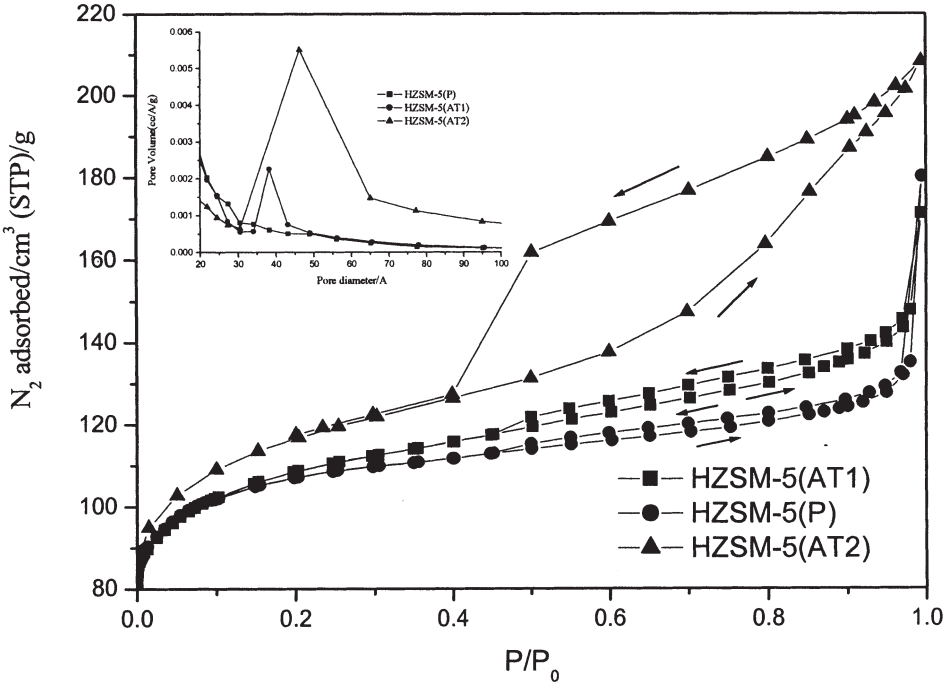

Figure 6. N_2 adsorption and desorption isotherms of the HZSM-5(P), HZSM-5(AT1) and HZSM-5(AT2) samples. The inlet is the mesopore distribution result of HZSM-5 before and after alkali treatment.

Table 4
Catalytic performance of 6 wt% Mo/HZSM-5(P) and alkali-treated 6 wt% Mo/HZSM-5 catalysts

Catalyst	CH_4 conversion (%)	Selectivity (%)						Yields of aromatics (%)
		Ben.	Tol.	Naph.	Lyx.	$C_2^=$	Coke	
Mo/HZSM-5(P)[a]	16.7	60.4	4.1	8.1	0.5	2.7	24.2	2.2
Mo/HZSM-5(P)[b]	3.9	37.7	3.9	1.5	0.5	23.2	33.2	1.7
Mo/HZSM-5(AT1)[a]	17.9	58.6	3.6	12.4	0.3	1.6	23.4	13.5
Mo/HZSM-5(AT1)[b]	11.6	68.6	6.3	4.5	0.9	6.7	13.0	9.3
Mo/HZSM-5(AT2)[a]	15.3	43.9	3.0	7.6	0.2	2.2	43.1	8.4
Mo/HZSM-5(AT2)[b]	4.9	37.7	5.1	1.3	0.8	15.6	39.5	2.2

Note: Reaction temperature: 1003 K; Reaction pressure: 1 atm; GHSV = 1500 mL/g/h.
[a]Data were taken at 60 min.
[b]Data were taken at 720 min.

236.2 eV, which was almost the same as the untreated 6Mo/HZSM-5 catalyst. This indicated that the molybdenum species are in the form of Mo^{6+}, which is in good agreement with the results reported by other authors [23–27]. This was evident that the alkali treatment did not cause any change in chemical state of the molybdenum species. The XPS spectra also suggested that there was certain amount of molybdenum species located on the external surface for both 6Mo/HZSM-5 and alkali-treated 6Mo/HZSM-5 catalysts. The near-surface composition of all the samples estimated from the corresponding XPS spectra is listed in table 5. The concentration of molybdenum species on the near-surface region is basically same on 6Mo/HZSM-5(P) and 6Mo/HZSM-5(AT1), while on 6Mo/HZSM-5(AT2) the concentration of molybdenum species on the near-surface region decreased largely. Because the bulk concentration of molybdenum species on the three fresh catalysts was almost the same as shown in table 5 by XRF, the XPS results suggested that the dispersion of molybdenum species on the catalyst surface was different before and after severe alkali treatment. When molybdenum species was loaded on HZSM-5 zeolite with moderate alkali treatment, the dispersion of molybdenum species did not change. But when the alkali treatment was too severe, the dispersion of molybdenum species on the zeolite decreased.

The result of NH_3-TPD profiles on 6Mo/HZSM-5(P) and 6Mo/HZSM-5(AT1) catalysts are shown in figure 9 and the corresponding deconvolution results are listed in table 6. Similar to what we have reported previously [28], there are three peaks centered at ca. 529, 584 and 721 K for the 6Mo/HZSM-5(P) catalysts and at ca. 538, 614 and 751 K for the 6Mo/HZSM-5(AT1) catalysts. All the peak temperatures shifted to the higher temperature side and the corresponding peak area increased in Peak

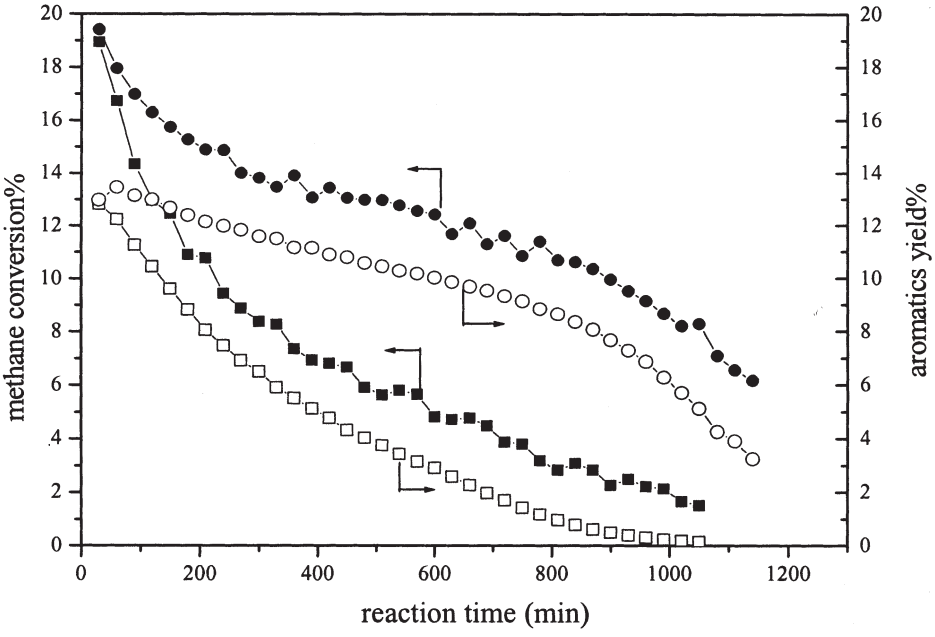

Figure 7. Methane conversion and aromatics yield on Mo/HZSM-5(P and AT1) catalysts versus time onstream (1003 K; 1 atm; GHSV = 1500 mL/g/h). The round and square symbol presents 6Mo/HZSM-5 (AT1) and 6Mo/HZSM-5 (P) respectively.

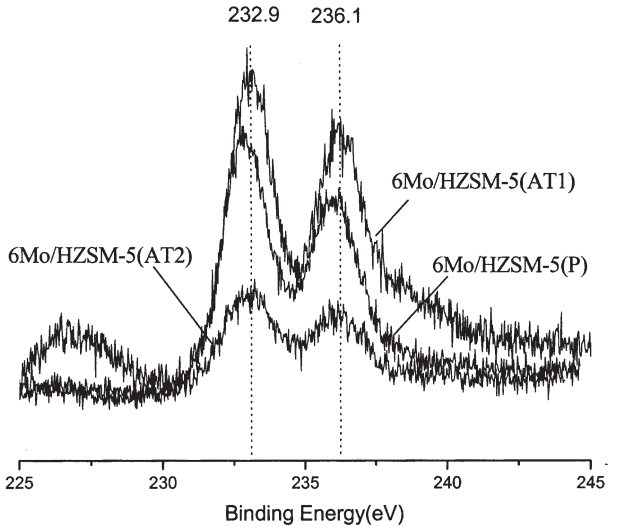

Figure 8. XPS spectra in Mo(3d) region recorded from fresh 6Mo/HZSM-5 (P, AT1 and AT2).

I, while the peak areas changed very little in Peak II and Peak III after the alkali modification. Although the acidity changed a little after the alkali treatment, the variation of acidity of the catalyst cannot explain the distinct difference of the reaction performance between 6Mo/HZSM-5(P) and 6Mo/HZSM-5(AT1) completely.

From the above results of ^{29}Si, ^{27}Al MAS NMR and N_2 adsorption and desorption experiments, we know that the alkali treatment of HZSM-5 zeolite creates another new kind of mesopores and at the same time the micropore system is still preserved. So, we believe that it is the change in the porosity after the alkali treatment that leads to the stability enhancement. The coexistence of the mesopores and the inherent micropores will be favorable for the MDA reaction from the point of view of mass transport. Methane activation and benzene formation need a channel structure of about 0.6 nm accommodating MoC*x* species, together with the presence of the Brønsted acid sites, as suggested by Iglesia recently [12]. With such a channel structure, the products of benzene and naphthalene thus formed must diffuse out of the channels effectively and timely; otherwise, they will be further condensed easily into polyaromatics and coke under the high temperature condition. Therefore, when a pore structure with the coexisting mesopores and micropores is created, not only can the aromatics product be selectively formed but they can also diffuse out of the zeolite channels easily

Table 5
Near-surface chemical compositions and total chemical compositions of fresh 6Mo/HZSM-5 and alkali-treated 6Mo/HZSM-5 samples determined by XPS[a] and XRF[b]

Samples	Mo[a] (wt%)	Mo[b]	O[b]	Si[b]	C[b]
6Mo/HZSM-5	6.2	6.5	59.6	16.9	17.0
6Mo/HZSM-5(AT1)	5.5	6.9	55.3	14.8	23.0
6Mo/HZSM-5(AT2)	6.8	1.3	67.7	23.4	7.7

[a]Determined by XRF experiment.
[b]Mo is estimated from Mo(3d), O from O(1s), Si from Si(2p) and C from C(1s) XPS spectra.

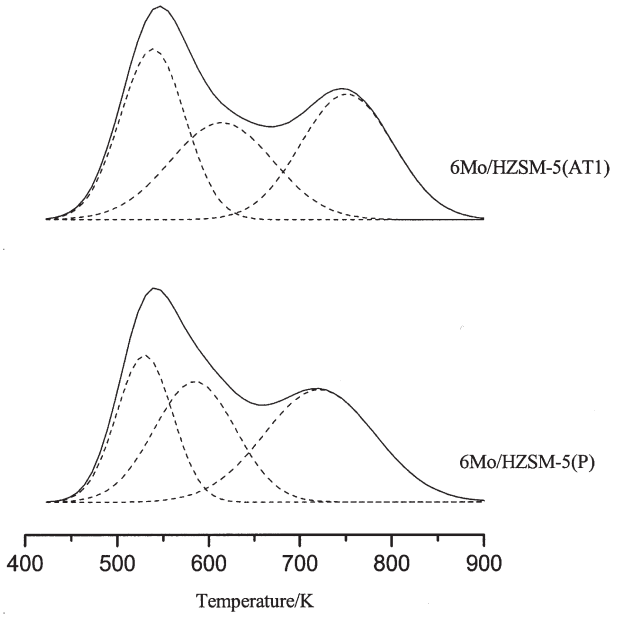

Figure 9. NH_3-TPD profiles of 6Mo/HZSM-5(P) and 6Mo/HZSM-5(AT1) catalysts.

due to the existence of the mesopores. Thus, the 6Mo/HZSM-5(AT1) catalysts, with the coexistence of mesopores and micropores on it, showed higher selectivity to aromatics and higher tolerance to carbonaceous deposits, leading to a better stability when compared with the conventional untreated 6Mo/HZSM-5(P) catalyst. But for the 6Mo/HZSM-5(AT2) catalysts, the condition is a little different. Although this catalyst also possesses the pore structure with coexisting mesopores and micropores, its original activity is much lower than the other two catalysts as shown in table 4. We think that there

Table 6
The deconvolution results of NH_3-TPD profiles of the 6Mo/HZSM-5(P) and 6Mo/HZSM-5(AT1) catalysts

Sample	Peak I		Peak II		Peak III	
	Temperature (K)	Area	Temperature (K)	Area	Temperature (K)	Area
6Mo/HZSM-5(P)	529	10 649	584	12 883	721	16 272
6Mo/HZSM-5(AT1)	538	14 180	613	13 139	751	15 026

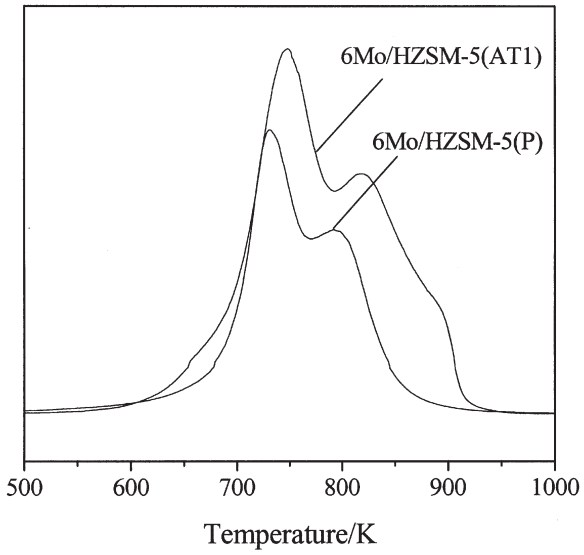

Figure 10. TPO profiles for the used 6Mo/HZSM-5(P) and 6Mo/HZSM-5(AT1) catalysts after running the reaction for 6 h at 1003 K.

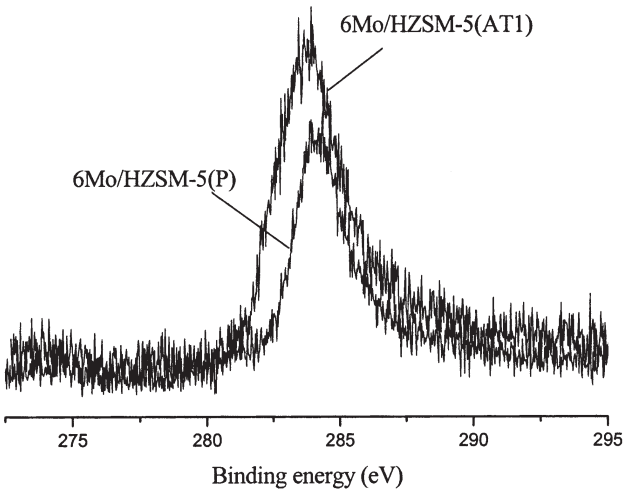

Figure 11. XPS spectra in C(1s) region recorded from the used 6Mo/HZSM-5 (P and AT1) catalysts after running the reaction for 6 h at 1003 K.

are several reasons leading to the appearance of this phenomenon. The first is due to the decrease of crystallization of the HZSM-5(AT2) because of the severe alkali treatment as shown in figure 1. The second is attributed to the decrease of molybdenum dispersion on the catalyst surface, which had been indicated in figure 8 and table 5. The third and the main reason is the pore distribution. Although on 6Mo/HZSM-5(AT2) catalyst there are two kinds of pores: micropore and mesopore, the ratio of these two kinds of pores is not favorable. After severe alkali treatment there was too much formation of mesopores and too much reduction of micropores as shown in figure 6 and table 3. In fact, inside the zeolite micropore channels, the methane conversion to aromatics will be enhanced and the polycondensation of aromatics rings forming carbon precursors will be kinetically limited by the zeolite shape selectivity. Appropriate amount of mesopores will benefit the diffusion of the reactants and products, but if the amount of mesopores is too large, it would reduce the aromatics selectivity because of the local loss of shape selectivity. So, although the existence of some mesopores is a benefit for the mass transformation, the ratio between micropores and mesopores must be appropriate. The detailed study of the balance between micropores and mesopores is in the process.

The investigation of the coked catalyst can also give some powerful evidence about the mesopore formation after the alkali treatment of zeolite. TPO profiles obtained on used 6Mo/HZSM-5(P) and 6Mo/HZSM-5(AT1) catalysts after running the reaction for 6 h are shown in figure 10 and the corresponding XPS spectra is shown in figure 11. We can clearly see that the amount of the coke deposited on 6Mo/HZSM-5(AT1) was larger than on 6Mo/HZSM-5(P) from the results of XPS and TPO. This result revealed that owing to the existence of mesopores on the 6Mo/HZSM-5(AT1) catalyst it could accommodate much larger carbonaceous deposits than the 6Mo/HZSM-5(P) catalysts.

4. Conclusions

Alkali treatment of HZSM-5 zeolite was performed and 6Mo/HZSM-5 catalysts were prepared by using the alkali-treated HZSM-5 zeolite. It was found that part of the siliceous species in the zeolite framework was dissolved after alkali treatment. So, the Si/Al ratio of the zeolite framework was decreased. On the other hand, there were no changes on the acid strength distribution and the number of the Brønsted acid sites after alkali treatment. The alkali treatment mainly altered the porosity and channel structure of the zeolite. A proper alkali treatment could create proper amount of mesopores, which coexisted with the inherent micropores of the HZSM-5 zeolite due to the dissolution of siliceous species of the zeolite framework. The 6Mo/HZSM-5 catalysts prepared by using alkali-treated HZSM-5 zeolite, with the coexistence of mesopores and micropores on it, showed higher selectivity to aromatics and higher tolerance to the carbonaceous deposits, thus leading to a remarkable enhancement of the reaction stability when compared with the conventional untreated 6Mo/HZSM-5 catalysts.

Acknowledgments

Financial supports from the Ministry of Science and Technology of China, the Natural Science Foundation of China, the Chinese Academy of Sciences and the BP-China Joint Research Center is gratefully acknowledged.

References

[1] L. Wang, T. Li, M. Xie and G. Xu, Catal. Lett. 21 (1993) 35.
[2] Y. Xu and L. Lin, Appl. Catal. A 188 (1999) 53.
[3] Y. Shu and M. Ichikawa, Catal. Today 71 (2001) 55.
[4] Y. Xu, X. Bao and L. Lin, J. Catal. 216 (2003) 386.
[5] D.M. Bibby, N.B. Milestone, J.E. Patterson and L.P. Aldridge, J. Catal. 97 (1986) 493.
[6] M. Guisnet and P. Magnoux, Appl. Catal. 54 (1989) 1.
[7] M. Guisnet and P. Magnoux, Stud. Surf. Sci. Catal. 88 (1994) 53.
[8] A. de Lucas, P. Canizares and A. Duran, Appl. Catal. A 206 (2001) 87.
[9] D. Wang, G.D. Meitzner and E. Iglesia, J. Catal. 206 (2002) 14.
[10] Y. Lu, D. Ma, X. Bao and L. Lin, J. Chem. Soc., Chem. Commum. (2002) 2048.
[11] D. Ma, Y. Lu, L. Su, Z. Xu, Z. Tian, Y. Xu, L. Lin and X. Bao, J. Phys. Chem. B 106 (2002) 8524.
[12] W. Richard, H. Young and E. Iglesia, J. Phys. Chem. B 103 (1999) 5787.
[13] B. Sharifah, H. Derouane-Abd, A.J. Ross and E.G. Derouane, Catal. Today 63 (2000) 461.
[14] C. Bouchy, I. Schmidt, J.R. Anderson, C.J.H. Jacobsen, E.G. Derouane and S.B. Derouane-Abd Hamid, J. Mol. Catal. A: Chem. 163 (2000) 283.
[15] C. Zhang, S. Li, Y. Yuan, W. Zhang, T. Wu and L. Lin, Catal. Lett. 56 (1998) 207.
[16] M. Ogura, S. Shinomiya, J. Tateno, Y. Nara and M. Matsukata, Chem. Lett. (2000) 882.
[17] M. Ogura, S. Shinomiya, J. Tateno, Y. Nara, M. Nomura, E. Kikuchi and M. Matsukata, Appl. Catal. A 219 (2001) 33.
[18] T. Suzuki and T. Okuhar, Microporous Mesoporous Mater. 43 (2001) 83.
[19] J.C. Groen, J. Perez-Ramirez and L.A. Peffer, Chem. Lett. (2002) 9.
[20] Y. Shu, D. Ma, X. Bao and Y. Xu, Catal. Lett. 66 (2000) 161.
[21] W. Liu, Y. Xu, S. Wong, J. Qiu and N. Yang, J. Mol. Catal. A 120 (1997) 257.
[22] D. Ma, Y. Shu, W. Zhang, X. Han, Y. Xu and X. Bao, Angew. Chem., Int. Ed. 39 (2000) 2928–2931.
[23] J. Shu, A. Adnot and B.P. Grandjean, Ind. Eng. Chem. Res. 38 (1999) 3860.
[24] D. Wang, M. Rosynek and J.H. Lunsford, Top. Catal. 3 (1996) 289.
[25] J.E. DeVries, H.C. Yao, R.J. Baird and H.S. Gandhi, J. Catal. 84 (1983) 8.
[26] P.E. Dai and J.H. Lunsford, J. Catal. 64 (1980) 173.
[27] T. Yang and J.H. Lunsford, J. Catal. 103 (1987) 55.
[28] Y. Shu, D. Ma, L. Xu, Y. Xu and X. Bao, Catal. Lett. 70 (2000) 67.